Generalization of the Keldysh theory of above-threshold ionization for the case of femtosecond pulses

Jonathan Parker and C. R. Stroud, Jr.
The Institute of Optics, University of Rochester, Rochester, New York 14627
(Received 28 November 1988; revised manuscript received 16 June 1989)

We develop a theory of the Keldysh-type appropriate for femtosecond excitation of atomic hydrogen. The new theory is tested by comparison with results of a direct numerical integration of the three-dimensional Schrödinger equation. In the case studied it is found that several of the standard approximations used in Keldysh calculations and in Fermi golden rule calculations are not valid. In particular, the slowly varying population approximation is not valid, and inhibition of ionization by coherent population trapping can occur.

I. INTRODUCTION

The first experimental observation of above-threshold ionization (ATI) a decade ago[1] has stimulated a great deal of work to develop the theory of the process by which an electron absorbs several extra photons beyond the minimum needed to ionize the atom to which it was initially bound. In some experiments more than 30 peaks have been seen in the spectrum of the electrons indicating the absorption of this many excess photons by the electron. The theory is complicated by the fact that ATI is fundamentally a high-order multiphoton process, by the fact that ATI is a saturated process in which successive order processes do not necessarily decrease in size, and by the fact that most ATI experiments have been carried out in xenon, an element with a rather complicated energy-level structure. Nevertheless, a certain class of theories has met with some success in modeling ATI cross sections. The most widely used theory was proposed by Keldysh[2] in 1965, and later modified by several authors.[3] The modified theory is now called the Keldysh-Faisal-Reiss (KFR) theory.

At present, work is going on to extend ATI experiments into the femtosecond regime and to atoms other than the noble gases.[4] Recently, Javanainen and Eberly[5] have compared several Keldysh models of the KFR type with the results of a numerical integration of a one-dimensional hydrogen atom, finding poor agreement between theory and numerical experiment. In the present paper we will develop a variant of the Keldysh theory appropriate for short pulses and test it by comparing its predictions with a direct numerical integration of the full three-dimensional Schrödinger equation for single-photon ionization of hydrogen.

The numerical integration of Schrödinger's equation reveals several new ATI effects. In order to use the numerical integration as a test of Keldysh theory it is necessary to understand these effects. The first effect is inhibition of ionization due to coherent population trapping. The result of this effect is that the electron is partially trapped in its initial bound state even though the fields are of exceptional intensity, 2.2×10^{14} W/cm^2. Second, we find that the slowly varying population approximation (SVPA) fails in this example of ATI. The failure of the SVPA will be discussed in Sec. V. The SVPA is used in the derivation of several theories of ATI, and in the derivation of Fermi's golden rule. Inhibition of ionization due to population trapping will be described in Sec. III.

In Sec. IV we will present a rigorous derivation of a variation of Keldysh theory beginning from Schrödinger's time-dependent equation. In Sec. IV we compare the proposed theory with the results of the numerical integration of Schrödinger's equation.

Several theories resembling Keldysh's original proposal have been discussed in the literature.[3,6,7] The best known modification to Keldysh's original proposal is the KFR theory. These theories are sometimes called Volkoff final-state theories for reasons that are explained in the Appendix. Here we adopt the more common practice[5] of calling them "theories of the Keldysh type." The theory developed in this paper yields formulas closely resembling the Keldysh formulas, although the derivation is very different. In the Appendix we compare the conventional (KFR) Keldysh predictions with the results of the numerical integration, and discuss the relationship between our theory and the conventional Keldysh theory.

II. NUMERICAL METHODS

Although typical ATI experiments require the absorption of many photons to ionize the atom, in the example that we investigate a single photon takes the electron from the initial state to the continuum of unbound states. The initial state is taken to be $n=3$, $l=2$, and $m=2$ in hydrogen. The peak intensity of the laser pulse is taken to be 2.2×10^{14} W/cm^2. The field is linearly polarized, with frequency equal to $\frac{1}{8}$ of the Rydberg frequency, with a Gaussian-shaped envelope and a duration of three optical periods full width at half maximum (FWHM). This choice of initial state and field polarization simplify the excitation in an important way. Because the dipole approximation is made throughout, the dipole selection rules for linearly polarized light forbid transitions from

the $l=2$, $m=2$ initial states to the $l=1$ states. This prevents, for example, a Rabi oscillation between the $n=3$, $l=2$ and the $n=2$, $l=1$ states that would greatly complicate the problem.

The numerical integration of Schrödinger's equation is carried out in the following fashion. The equation is integrated on a complete set of states, the set of eigenstates of the Hamiltonian of a hydrogen atom in a spherical potential well. It is assumed that the atom is at the center ($r=0$) and that there is an infinite spherical potential barrier at radius $r=R$. The resulting set of states is complete for solutions of Schrödinger's equation satisfying the boundary conditions $r\Psi(r)=0$ at $r=0$ and $r=R$. To guarantee that $r\Psi(r)=0$ at $r=R$, we verify that the wave packet representing the ionized electron has not reached the boundary $r=R$ at the end of the pulse. The problem, then, is a well understood Sturm-Liouville problem. We make the dipole approximation and neglect the ponderomotive forces. These are the only significant simplifications. The dipole approximation is well justified in the regime we will study. Ponderomotive effects, which are due to large gradients in the electric field strength, can greatly modify ATI spectra. These effects are strongly dependent on experimental parameters and are largely classical. We will simplify our theory by omitting this effect, which can be easily grafted on to describe a particular experimental situation.

The advantage of integrating the equation on a complete set of discrete, physical state is that bound states may be removed from the set during the integration to see what effect they have on the ATI energy spectrum. This tells us unambiguously the origin of effects such as the inhibition of ionization. Using a physical basis set and knowing which bound states are of importance during the excitation allows us also to generalize results to other one-electron atoms. It is easily seen from the energy-level diagrams of lithium and sodium that the results would differ little in the $m=2$ case if the atom were lithium or sodium. In recent years, another numerical method, the Sturmian method, has become increasingly popular in problems of the sort discussed here. It should be noted that the Sturmian basis states are not equivalent to the hydrogenic basis states drawn in Fig. 1. A recent review of the advantages and disadvantages of the two methods is given by Susskind and Jensen.[8]

The energy-level diagram is drawn in Fig. 1. For each azimuthal quantum number l there are an infinite number of states. The positive-energy states do not form a continuum but are at discrete energies due to the cavity boundary conditions. To make the diagram more legible every fifth positive energy state is plotted. In Fig. 1 the thick arrows are a photon's length in energy and are drawn to represent the most probable path that population takes during the excitation. The population also follows the thin lines, but these excitation paths do not contribute significantly to the final spectrum.

More than 1600 states ($l=2$, 3, 4, 5, and 6) are used in the integration. Many more states than are necessary for the integration are kept in the basis. In particular, we keep states of high energy and high angular momentum that receive negligible population and that can only receive population through many-photon transitions. To produce the result shown here the step size of the time integration is made sufficiently small that the wave function Ψ remains normalized to ten significant figures throughout the integration. We then repeated the numerical integrations with a smaller step size, so that the wave function remained normalized to 15 significant figures. The results remained unchanged.

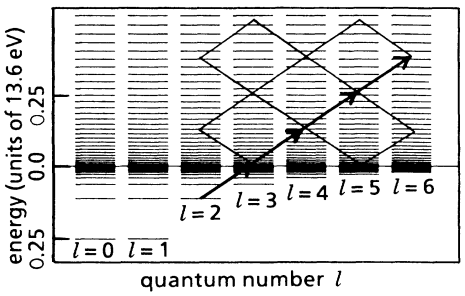

FIG. 1. Energy-level diagram for the numerical integration of Schrödinger's equation. The thick arrows represent the most probable paths taken by population during the excitation. The population also follows the thin lines these paths contribute insignificantly because of the smaller dipole moments. One in five of the unbound states are plotted. Altogether over 1600 states were used.

III. NUMERICAL RESULTS

In this section we will discuss some of the complications and effects revealed by the numerical integration. It is necessary to understand these complications in order to test the Keldysh-type theories in subsequent sections.

In Fig. 2 we have plotted the results of integrating Schrödinger's equation. The solid curve represents the energy distribution of the electron at the end of the pulse. The curve is constructed by dividing each photon-energy interval (of energy $\frac{1}{8}$ Rydberg) into ten bins. The amount of population in each bin is plotted in Fig. 2. The bound states are drawn as rectangles; the population in unbound states (the ATI spectrum) is plotted with a smooth curve rather than a histogram to make comparison with the other theories easier. There are four ionization peaks, although the fourth, with 0.09% of the population, is not visible in the figure.

In Fig. 3 is plotted (solid line) the population of the initial state ($n=3$, $l=2$, $m=2$) during the pulse. The pulse peaks in intensity at $t=0$ and has a FWHM of $3T_\omega$, where T_ω is the period of the electric field. From Fig. 3 it is evident that when the pulse is the most intense ($t=0\pm1.5T_\omega$) almost no net population leaves the initial state. The rapid oscillations in the population of the initial state have frequency of twice the optical frequency of the electric field. There are counter-rotating oscillations that are normally discarded in the rotating-wave approximation.

This inhibition of ionization may be characterized as an intense-field modification of the Fermi golden rule

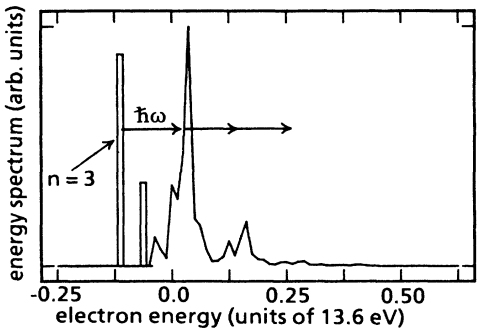

FIG. 2. Electron energy at the end of the excitation pulse. The separation of the x axis hash marks is one photon in energy: $\frac{1}{8}$ Ry. The curves are constructed by dividing each energy interval of $\frac{1}{8}$ Ry into ten bins. Population in each bin is plotted with a rectangle for the bound states $n=3$ and $n=4$, and a solid line otherwise. Here the initial state is $n=3$, $l=2$, $m=2$ and the peak intensity of the laser pulse is 2.2×10^{14} W/cm^2.

(FGR). For comparison, the FGR prediction is also plotted (dashed line). The FGR rate of exponential decay is calculated by assuming a single $l=2$ bound state and a single $l=3$ continuum of unbound states. A simple FGR calculation predicts complete ionization at intensities an order of magnitude lower than the 2.2×10^{14} W/cm^2 peak intensity actually used.

The origin of the inhibited ionization may be easily demonstrated by removing basis states from the basis set

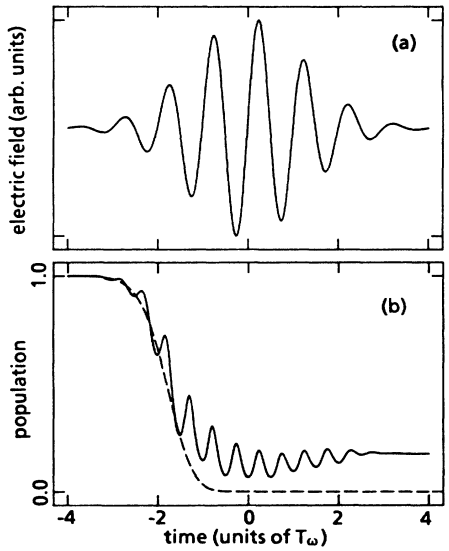

FIG. 3. (a) Laser pulse electric field. The pulse has a Gaussian envelope, and the optical frequency ω is 13.6 eV/(8$\hbar$). The pulse has a FWHM of $3T_\omega$. T_ω is the period of the optical field. (b) Population in the initial ($n=3$, $l=2$, $m=2$) state during the laser pulse. The solid line shows the initial-state population predicted by the numerical integration of Schrödinger's equation. The dashed line shows the initial-state population predicted by Fermi's golden rule.

during the integration. If the states ($n=4$, $l=2$, $m=2$) and ($n=5$, $l=2$, $m=2$) are removed from the basis set, then the initial state decays nearly as predicted by FGR. Absorption of population by the $n=4$ and 5 states (via the $l=3$ continuum of unbound states) then, in effect inhibits ionization. To see how population trapping modifies the excitation, consider the equation of motion of a state $|n\rangle$ in the first ionization peak. Let Ψ_i be the superposition of the three $l=2$ bound states of principal quantum number 3, 4, and 5. Then the coupling of the ($l=3$) state $|n\rangle$ to the initial ($l=2$) coherent state Ψ_i is governed by

$$i\hbar\frac{da_n}{dt}=\exp(i\omega_n t)\left[-\frac{e}{mc}A_z(t)\right]\langle n|p_z|\Psi_i(t)\rangle\ . \tag{1}$$

Here a_n is the probability amplitude of a state $|n\rangle$ at the center of the first ($l=3$) ionization peak and $A_z(t)$ is the field potential. A numerical calculation demonstrates that the quantity $\langle n|p_z|\Psi_i(t)\rangle$ falls rapidly to near zero as the pulse peaks in intensity ($t=0\pm1.5T_\omega$). Population flows into the $n=4$ and 5 bound states ($l=2$) in such a way as to effectively turn off the transition from the $l=2$ bound states to the $l=3$ unbound states. In other words, a ($l=2$) coherent state Ψ_i is generated that exhibits a greatly reduced ionization cross section in comparison to the FGR prediction. Numerically, it is found that the effect seems to occur naturally at intensities both higher (9×10^{14} W/cm^2) and lower (5×10^{13} W/cm^2) than in the example used here. In fact, at 9×10^{14} W/cm^2 more population remains in the $n=3$ initial state at the end of the pulse than at the end of a 5×10^{13} W/cm^2 pulse.

The results may seem surprising, but the principal features may be modeled both numerically and theoretically with a simple model employing just the $l=3$ ionization continuum and a few $l=2$ bound states. We have recently completed a theory of inhibited ionization[9] in intense fields that gives good agreement with the principal features of the full numerical integration described in this paper. The theory demonstrates that for a wide variety of atomic-level spacings, laser pulse shapes, field intensities, and atomic dipole moments, a coherent state Ψ_i may be generated that exhibits a greatly reduced ionization cross section in comparison to the FGR prediction.

Recently, Eberly and Javanainen,[10] and Sundaram and Armstrong[11] have discussed the role that excited bound states play in modifying the ATI peak shapes. Inhibition of ionization and population trapping due to coherences among two or more bound states has been extensively studied both in the theory of two-color ionization[12] and in the theory of one-color ionization.[13]

IV. KELDYSH THEORY FROM TIME-DEPENDENT QUANTUM MECHANICS

A general theory of the Keldysh type can be derived in a few steps from the time-dependent Schrödinger equation. The derivation is aided by experience with the basis-state method described above.

The first step is to break the wave function into two

parts, the initial state Ψ_i defined above, and the final state Ψ_f. By Ψ_f we mean the coherent superposition of all positive-energy states. This subset of the complete set of states of Fig. 1 was chosen because experience with the numerical integration indicated that discarded states play little direct role in the excitation. Then Schrödinger's equation is

$$i\hbar\frac{d\Psi_f}{dt}=[\hat{H}_0+\hat{H}_{\rm int}(t)]\Psi_f + \left[\hat{H}_0+\hat{H}_{\rm int}(t)-i\hbar\frac{d}{dt}\right]\Psi_i \ , \tag{2}$$

where $\hat{H}_0$ is the atomic Hamiltonian and $\hat{H}_{\rm int}(t)$ is $-e\hat{\mathbf{p}}\cdot A/mc+e^2\mathbf{A}\cdot\mathbf{A}/2mc^2$.

Now writing the final state as $\sum_p c(\mathbf{p},t)|\mathbf{p}\rangle$, a superposition of plane-wave states, and taking the projection of Eq. (2) on $\langle\mathbf{p}|$ yields

$$i\hbar\frac{dc(\mathbf{p},t)}{dt}=\langle\mathbf{p}|\hat{H}_0|\Psi_f\rangle + \left[-\frac{e}{mc}\mathbf{A}\cdot\mathbf{p}+\frac{e^2}{2mc^2}\mathbf{A}\cdot\mathbf{A}\right]c(\mathbf{p},t) + \left\langle\mathbf{p}\left|\hat{H}_0+\hat{H}_{\rm int}-i\hbar\frac{d}{dt}\right|\Psi_i(t)\right\rangle \ . \tag{3}$$

The effect of taking the projection of the equation on $\langle\mathbf{p}|$ was to replace the canonical momentum operator $\hat{\mathbf{p}}$ in the interaction Hamiltonian $H_{\rm int}$ with a c number $\mathbf{p}$. At the end of the pulse, $\mathbf{p}$ is the physical momentum of the ionized electron.

The most important approximation in the derivation will be called the "plane-wave approximation." By the plane-wave approximation we mean that

$$\langle\mathbf{p}|\hat{H}_0|\Psi_f\rangle=\left\langle\mathbf{p}\left|\frac{\hat{\mathbf{p}}\cdot\hat{\mathbf{p}}}{2m}+V(r)\right|\Psi_f\right\rangle\simeq\frac{\mathbf{p}\cdot\mathbf{p}}{2m}\langle\mathbf{p}|\Psi_f\rangle \ . \tag{4}$$

The assumption is, then, that the Coulomb potential perturbs the final states insignificantly. The plane-wave approximation is closely related to the zeroth-order Born approximation. It is well known[14] that the first-order correction to the zeroth-order Born approximation is small in transitions from an initial bound state of quantum number l to final unbound states of quantum number $l+1$.

With this approximation, Eq. (3) may be immediately integrated to give

$$|c(\mathbf{p},t)|^2=\left|\frac{1}{\hbar}\int_{-\infty}^{t}dt'\exp\left[\frac{i}{\hbar}\int_{-\infty}^{t'}dt''\left[\frac{\mathbf{p}\cdot\mathbf{p}}{2m}+H_{\rm int}(t'')\right]\right]\left\langle\mathbf{p}\left|\hat{H}_0+H_{\rm int}-i\hbar\frac{d}{dt'}\right|\Psi_i(t')\right\rangle\right|^2 \ . \tag{5}$$

In the interaction Hamiltonian of Eqs. (2)–(5) we have kept the $\mathbf{A}\cdot\mathbf{A}$ term even though a simple transformation might have removed it from the dipole-approximation Schrödinger equation at the start. In the dipole approximation, the $\mathbf{A}\cdot\mathbf{A}$ term has no effect on the ATI spectrum. If Ψ is a solution of the Schrödinger equation with the $\mathbf{A}\cdot\mathbf{A}$ term, and if $\tilde{\Psi}$ is a solution of the Schrödinger equation without the $\mathbf{A}\cdot\mathbf{A}$ term, then Ψ and $\tilde{\Psi}$ are related by a simple transformation

$$\tilde{\Psi}(r,t)=\exp\left[\frac{i}{\hbar}\int_{-\infty}^{t}dt'\left[\frac{e^2\mathbf{A}(t')\cdot\mathbf{A}(t')}{2mc^2}\right]\right]\Psi(r,t) \ . \tag{6}$$

The gauge transformation, Eq. (6), is sometimes called a contact transformation.

The Schrödinger equation for Ψ and the Schrödinger equation for $\tilde{\Psi}$ predict (in the absence of approximations beyond the dipole approximation) the same physical results. Next in this section we will show that our theory [Eq. (5)], with its approximations, predicts the same physical results whether it is derived from the Schrödinger equation for Ψ or the Schrödinger equation for $\tilde{\Psi}$. This corrects a well known[15,16] defect in the conventional Keldysh theory, which gives different physical predictions depending on whether it is derived from the Schrödinger equation for Ψ or the Schrödinger equation for $\tilde{\Psi}$.

Let us now transform Eq. (5), using Eq. (6), to get a formula for $c(\mathbf{p},t)$ that uses $\tilde{\Psi}_i$ instead of Ψ_i. Setting $\Psi_i=\exp[-i(e^2/2mc^2\hbar)\int^t\mathbf{A}\cdot\mathbf{A}]\tilde{\Psi}_i$, and using

$$\exp\left[\frac{i}{\hbar}\int_{-\infty}^{t}dt'\left[\frac{e^2\mathbf{A}\cdot\mathbf{A}}{2mc^2}\right]\right]\left[\frac{e^2\mathbf{A}\cdot\mathbf{A}}{2mc^2}-i\hbar\frac{d}{dt}\right] \times\exp\left[-\frac{i}{\hbar}\int_{-\infty}^{t}dt'\left[\frac{e^2\mathbf{A}\cdot\mathbf{A}}{2mc^2}\right]\right]\tilde{\Psi}=-i\hbar\frac{d}{dt}\tilde{\Psi} \ , \tag{7a}$$

yields

$$|c(\mathbf{p},t)|^2=\left|\frac{1}{\hbar}\int_{-\infty}^{t}dt'\exp\left[\frac{i}{\hbar}\int_{-\infty}^{t'}dt''\left[\frac{\mathbf{p}\cdot\mathbf{p}}{2m}-\frac{e\mathbf{p}\cdot\mathbf{A}}{mc}\right]\right] \times\left\langle\mathbf{p}\left|\hat{H}_0-\frac{e\mathbf{p}\cdot\mathbf{A}}{mc}-i\hbar\frac{d}{dt'}\right|\tilde{\Psi}_i(t')\right\rangle\right|^2 . \tag{7b}$$

Equations (5) and (7b) are equivalent and must give the same predictions if properly evaluated. Equation (6) may be thought of simply as a change of variables to simpify the numerical integration of Eq. (5).

Equation (7b) is just the formula that would have followed from a Schrödinger equation that had no $\mathbf{A}\cdot\mathbf{A}$

term in the interaction Hamiltonian. We have shown, then, that our theory gives the same physical predictions whether it is derived from the Schrödinger equation for Ψ or that for $\tilde{\Psi}$. This is true because we kept the operator d/dt in the matrix elements of Eqs. (5) and (7b). If, by contrast, we were to discard the d/dt term in Eq. (5), then such a theory, if it were derived from the Schrödinger equation for Ψ, would give physical predictions different from those of a theory derived from the Schrödinger equation for $\tilde{\Psi}$. In Sec. V we will show how to remedy this problem in an approximation in which the d/dt operator is discarded.

To make a quantitative comparison between the numerical integration of Schrödinger's equation and the formulas derived above we will use the numerically integrated initial state $\Psi_i(t)$ defined in Sec. III. In practice we solve Schrödinger's equation without the $\mathbf{A}\cdot\mathbf{A}$ term to get $\tilde{\Psi}_i$ directly, and then use Eq. (7b). To get an energy spectrum we sum all of the plane-wave states $|\mathbf{p}\rangle$ in each energy interval $(E, E+dE)$, where dE is the bin width of the spectrum of Fig. 2. This is a standard method of calculating a cross section with the Born approximation. A good textbook discussion of its justification is given by Gottfried.[17] The approximation is good except near the $E=0$ ionization threshold. At the $E=0$ ionization threshold the density of plane-wave states goes to zero, whereas the true density of states does not go to zero at $E=0$.

In Fig. 4 we plot (dotted line) the results of our full theory: the energy spectrum predicted by Eq. (7b). The agreement is good enough to give us confidence in our numerical methods. The third and fourth Keldysh ionization peaks have the wrong side-lobe structure in comparison to the numerical integration, but the right cross section and shape for the central part of the peak.

The theory presented here, Eq. (7b), is basically Schrödinger's equation in the momentum picture simplified by two approximations. The first approximation was to discard from the basis set of Fig. 1 some unimportant states. Experience with the numerical integration suggests that this approximation is very good. The second approximation is the plane-wave approximation, Eq. (4). Finally, in using Eq. (7b) to calculate a cross section, the plane-wave density of states is used. This approximation is good except near the threshold of ionization.[17]

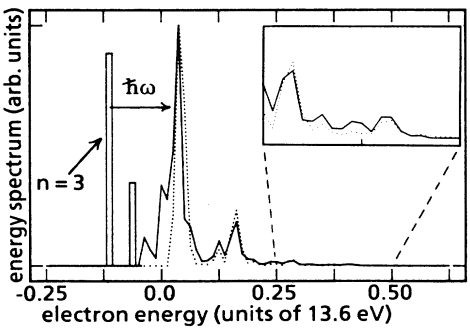

FIG. 4. Electron energy at the end of the laser pulse. The solid line is the prediction of numerically integrating Schrödinger's equation. The dotted line is the prediction of the Keldysh-type theory proposed here, Eq. (7).

V. SLOWLY VARYING POPULATION APPROXIMATION

In Sec. IV we used the numerically integrated initial state $\Psi_i(t)$ in order to test how well Eq. (7b) predicts the ATI spectrum. This strategy was useful in testing theory, but the strategy is not of much use in modeling experiments. In order to make the theory of practical value in situations where Schrödinger's equation has not been or cannot be integrated, it is necessary to use an approximate Ψ_i. In this section we will review a standard approach to choosing an approximate Ψ_i, which we will call the slowly varying population approximation. The results of this section are also necessary in order to compare our theory with the standard Keldysh theories, which are formulated in the slowly varying population approximation.

By the slowly varying population approximation we mean the assumption that the population of the initial state remains constant during the excitation, or is slowly varying. This approximation is commonly made in order to use formulas such as Eq. (7b) to calculate transition rates, or equivalently cross sections. To see the effect of this approximation of Eq. (7b), consider the operator $\hat{H}_0 - i\hbar d/dt$ in the matrix element of Eq. (7b). This operator, acting on any state yields

$$\left[\hat{H}_0 - i\hbar\frac{d}{dt}\right]\sum_i a_i(t)\exp(-iE_i t/\hbar)|i\rangle = \frac{\hbar}{i}\sum_i \frac{da_i(t)}{dt}\exp(-iE_i t/\hbar)|i\rangle \ . \quad (8)$$

In Eq. (8), H_0 is the atomic Hamiltonian, E_i is the energy of the ith state, and the $a_i(t)$ are the probability amplitudes of the states. In the slowly varying population approximation it is assumed that each amplitude $a_i(t)$ is constant in time or so slowly varying that da_i/dt is negligible. By the slowly varying population approximation we mean, then, that $\hat{H}_0 - i\hbar d/dt$ disappears from the matrix element of Eq. (7b).

In Sec. IV it was pointed out that conventional Keldysh theory predicts different physical results, depending on whether it is derived from the Schrödinger equation for Ψ or from the Schrödinger equation for $\tilde{\Psi}$. This difficulty is avoided if the slowly varying population approximation is correctly applied.

The next step is to apply the slowly varying population approximation to Eq. (5). Since the interaction Hamiltonian now has the $\mathbf{A}\cdot\mathbf{A}$ term in it, we apply the transformation Eq. (6) to the wave function of Eq. (8). Consider the operator $\hat{H}_0 - i\hbar d/dt + e^2\mathbf{A}\cdot\mathbf{A}/2mc^2$ acting on that state

$$\left[\hat{H}_0 - i\hbar\frac{d}{dt} + \frac{e^2\mathbf{A}\cdot\mathbf{A}}{2mc^2}\right]\sum_i a_i(t)\exp\left[-\frac{i}{\hbar}\int_{-\infty}^{t} dt'\left[\frac{e^2\mathbf{A}\cdot\mathbf{A}}{2mc^2}\right]\right]\exp(-iE_i t/\hbar)|i\rangle$$

$$= \frac{\hbar}{i}\sum_i \frac{da_i(t)}{dt}\exp\left[-\frac{i}{\hbar}\int_{-\infty}^{t} dt'\left[\frac{e^2\mathbf{A}\cdot\mathbf{A}}{2mc^2}\right]\right]\exp(-iE_i t/\hbar)|i\rangle \ . \quad (9)$$

If the $\mathbf{A}\cdot\mathbf{A}$ term is in the interaction Hamiltonian, then the slowly varying quantity is the amplitude $a_i(t)$ of Eq. (9) [assuming that $a_i(t)$ is the slowly varying quantity of Eq. (8)]. Consequently, the slowly varying population approximation applied to Eq. (5) means that $da_i(t)/dt$ is negligible and $\hat{H}_0 - i\hbar d/dt + e^2\mathbf{A}\cdot\mathbf{A}/2mc^2$ is discarded from the matrix element of Eq. (5). As a result, application of the slowly varying population approximation to Eq. (5) yields exactly the same formula that application of the slowly varying population approximation to Eq. (7b) yielded.

To actually model experiments, or calculate cross sections, a further approximation is usually made: it is assumed that the population remains entirely in a single bound state rather that the three that make up the $\Psi_i(t)$ used in Sec. IV. This further approximation will not be investigated here. Instead the numerically integrated $\Psi_i(t)$ will be used in our test of the theory.

The slowly varying population approximation and its consequence in Eq. (7b), $\hat{H}_0 - i\hbar d/dt = 0$, are made so commonly in the theory of multiphoton processes that it is worthwhile to investigate its validity here. It is also used in the standard Keldysh approach, the KFR theory, to be discussed in the Appendix. So, in order to compare our theory, Eq. (7b), with the KFR theory, we must apply the slowly varying population approximation to Eq. (7b). To do this, we remove $\hat{H}_0 - i\hbar d/dt$ from the matrix element of Eq. (7b) and plot the results.

In Fig. 5 is shown (dotted line) the energy spectrum predicted by Eq. (7b) with the $\hat{H}_0 - i\hbar d/dt$ operator discarded. The ionization peaks predicted by the theory are in the right places, but the cross section of the first Keldysh peak is wrong by a factor of 2 and the cross section of the second Keldysh peak is wrong by a factor of 4.

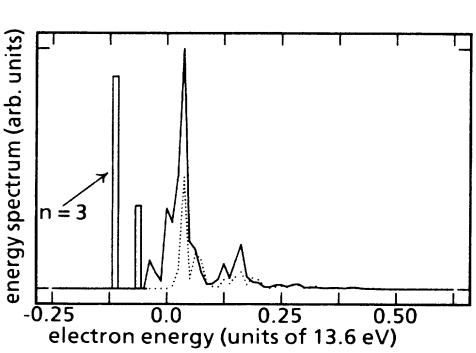

FIG. 5. Electron energy at the end of the laser pulse. The solid line is the prediction of numerically integrating Schrödinger's equation. The dotted line is the prediction of the Keldysh-type theory proposed here [Eq. (7)] in the slowly varying population approximation.

The d/dt operator plays such an important role in Eq. (7b) because of the rapid oscillations in ground-state decay, as shown in Fig. 3. These rapid oscillations have a frequency of twice the frequency of the electric field. They are sometimes called counter-rotating oscillations because they are due to rapidly oscillating terms in Schrödinger's equation that are discarded in the rotating-wave approximation (RWA). In terms of Eq. (8), the rapid oscillations mean that the functions $a_i(t)$ have parts that go as $\sin(2\omega t)$ where ω is the optical frequency. As a consequence, $\hat{H}_0 - i\hbar d/dt$ gives a large contribution in Eq. (7b).

VI. CONCLUSIONS

We have derived directly from Schrödinger's equation a very general formula of the Keldysh type. The general formula is valuable in two respects. First, it is this general formula that makes possible a useful comparison of Keldysh theory with the results of the numerical integration of Schrödinger's equation. The general Keldysh theory agrees in some respects with numerical integration and disagrees in others. The comparison is in effect a numerical test of the first two major approximations necessary to derive Keldysh-type theories. The general formula is valuable in another respect. It allowed us to correct a well-known[15,16] defect in the standard KFR Keldysh theory. The standard theory gives different physical predictions depending on whether it is derived from the Schrödinger equation with the $\mathbf{A}\cdot\mathbf{A}$ term or alternately from the Schrödinger equation without the $\mathbf{A}\cdot\mathbf{A}$ term. We have shown that our theory gives the same physical predictions in either case. We have further shown how to preserve this invariance in the limit of the slowly varying population approximation.

Next we have discussed at length the slowly varying population approximation. We have done this for two reasons. The first season was to test the agreement of our Keldysh theory in this limit with the numerical integration. This is important because so much of the theory of multiphoton processes is done in the SVPA. The second reason is that the standard Keldysh theory is in the SVPA, and so the SVPA is the limit in which our Keldysh may be compared with standard KFR Keldysh theory. We have shown that ours is not equivalent to the standard KFR theory (Appendix A). It is by this set of steps that we have shown how to derive theories of the Keldysh type directly from Schrödinger's time-dependent equation, and it is by this set of steps that we have nu-

merically tested the series of approximations necessary to derive the theories.

Perhaps the most important characteristic shared by all the theories of the Keldysh type is the plane-wave approximation, Eq. (4). Equation (7b) is very nearly Schrödinger's equation, simplified only by the plane-wave approximation; the essential states approximation in this case is a very good approximation.

ACKNOWLEDGMENTS

We would like to thank A. Szöke and J. N. Bardsley for useful discussions. We would like to acknowledge support by the Joint Service Optics Program and by the U.S. Army Research Office.

APPENDIX

In this Appendix we will write down the standard Keldysh formula describing ATI of atoms in intense fields, namely the KFR theory, of Keldysh, Faisal, and Reiss. The standard formula will be compared with the formula derived in Sec. IV and with the numerical solution of Schrödinger's equation. We will show that the two theories predict different results.

A physically appealing[6] derivation of the transition probability $|M_{fi}|^2$ describing an ATI transition in intense fields assumes that a single matrix element connects the initial atomic bound state Ψ_i to an unbound (dressed) state Ψ_f. The final state $\Psi_f(\mathbf{p},\mathbf{r},t)$ is assumed to be the Volkoff state, an exact solution of Schrödinger's equation for an unbound electron in a time-varying electric field. With these assumptions the probability of scattering a bound electron into a plane wave $\Psi_f(\mathbf{p},\mathbf{r},t)$ of momentum $\mathbf{p}$ is

$$|M_{fi}(\mathbf{p})|^2=\left|\frac{1}{\hbar}\int_{-\infty}^{\infty}dt'\langle\Psi_f(\mathbf{p},\mathbf{r},t)|H_{\rm int}(t')|\Psi_i(r,t')\rangle\right|^2, \tag{A1}$$

where $H_{\rm int}$ is the interaction Hamiltonian. The Volkoff state is

$$\Psi_f(\mathbf{p},r,t)=\Psi_0\exp(i\mathbf{p}\cdot\mathbf{r}/\hbar)\times\exp\left[-\frac{i}{\hbar}\int_{-\infty}^{t}dt'\left[\frac{\mathbf{p}\cdot\mathbf{p}}{2m}+H_{\rm int}(t')\right]\right], \tag{A2}$$

where Ψ_0 is the inverse of the square root of the quantization volume. The published Keldysh-type theories share a form similar to Eq. (A1). Reiss[3] derives an equivalent formula from scattering theory. The equation is, in our notation,

$$|c(\mathbf{p},t)|^2=\left|\frac{1}{\hbar}\int_{-\infty}^{t}dt'\exp\left[\frac{i}{\hbar}\int_{-\infty}^{t'}dt''\left[\frac{\mathbf{p}\cdot\mathbf{p}}{2m}+H_{\rm int}(t'')\right]\right]\langle\mathbf{p}|H_{\rm int}(t')|\Psi_i(t')\rangle\right|^2. \tag{A3}$$

In Eqs. (A1)–(A3) the interaction Hamiltonian $H_{\rm int}$ is $-e\mathbf{p}\cdot\mathbf{A}/mc+e^2\mathbf{A}\cdot\mathbf{A}/2mc^2$.

Now it is straightforward to see the relationship between our theory, Eq. (5), and the KFR theory, Eq. (A3). In the KFR theory,[4] a cross section or rate is calculated from Eq. (A3) by choosing the initial state Ψ_i to be a single bound state of constant population $\Psi_i=\exp(-iE_it/\hbar)|i\rangle$. One can readily verify that substituting this initial state into Eq. (5) yields Eq. (A3).

To further clarify the differences between our theory and the KFR theory, we will show how to us our theory, Eqs. (5) and (7b), to calculate an ionization cross section from an initial bound state of constant population $|i\rangle$. It follows from the discussion of Secs. IV and V that the proper initial state of constant population to put into Eq. (5) to get an ionization cross section is

$$\Psi_i=\exp[-i(e^2/2mc^2\hbar)\int^t\mathbf{A}\cdot\mathbf{A}]\exp(-iE_it/\hbar)|i\rangle\ .$$

The proper initial state of constant population to put into Eq. (7b) is $\tilde{\Psi}_i=\exp(-iE_it/\hbar)|i\rangle$. To get the KFR equation and the related Keldysh formulas, we must put $\tilde{\Psi}_i=\exp(-iE_it/\hbar)|i\rangle$ into Eq. (5). Still another way to characterize the difference between the theories is this: our theory uses the dressed initial state; the KFR uses the initial atomic state unperturbed by external fields.

It was shown in Sec. V that the slowly varying population approximation fails in the example of ATI discussed here. The approximation, however, is successful in a wide class of problems and, in particular, may be useful in modeling other examples of ATI. For these reasons, it

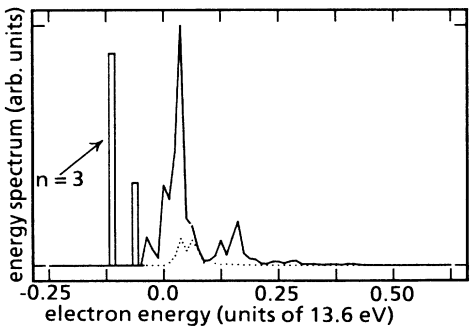

FIG. 6. Electron energy at the end of the laser pulse. The solid line is the prediction of numerically integrating Schrödinger's equation. The dotted line is the prediction of conventional Keldysh theory.

is worth comparing the predictions of our theory, Eq. (7b) (in the slowly varying population approximation) with the KFR theory. We will show that the two theories give different predictions. The prediction of our theory is given in Fig. 5, and described in Sec. V. In Fig. 6 is shown (dotted line) the prediction of Eq. (A3). The initial state $\Psi_i(t)$, used in Eq. (A3) is as defined in Sec. III, the coherent superposition of three bound states. Comparison of Fig. 5 (our theory) and Fig. 6 shows that the theories predict different spectra.

[1]P. Agostini, F. Fabre, G. Mainfray, G. Petite, and N. Rahman, Phys. Rev. Lett. **42**, 1127 (1979).

[2]L. V. Keldysh, Zh. Eksp. Teor. Fiz. **47**, 1945 (1964) [Sov. Phys.—JETP **20**, 1307 (1965)].

[3]A. I. Nikishov and V. I. Ritus, Sov. Phys. **23**, 168 (1966); F. Faisal, J. Phys. B **6**, L312 (1973); H. R. Reiss, Phys. Rev. A **22**, 1786 (1980).

[4]D. Feldmann, B. Wolff, M. Wemhoner, and K. H. Welge, Z. Phys. **6**, 293 (1987).

[5]J. Javanainen and J. H. Eberly, J. Phys. B **21**, L93 (1988); Phys. Rev. A **39**, 458 (1988).

[6]W. Becker, R. R. Schlichter, M. O. Scully, and Wodkiewicz K, J. Opt. Soc. Am. B **4**, 743 (1987).

[7]J. Kupersztych, Europhys. Lett. **4 (1)**, 23 (1987).

[8]S. M. Susskind and R. V. Jensen, Phys. Rev. A **38**, 711 (1988).

[9]J. Parker and C. R. Stroud, Jr. (unpublished).

[10]J. H. Eberly and J. Javanainen, Phys. Rev. Lett. **60**, 1346 (1988).

[11]Bala Sundaram and Lloyd Armstrong, Jr., Phys. Rev. A **38**, 152 (1988).

[12]H. R. Gray, R. M. Whitley, and C. R. Stroud, J. Opt. Lett. **3**, 218 (1978); P. L. Knight, Opt. Commun. **31**, 148 (1979); P. E. Coleman and P. L. Knight, J. Phys. B **15**, 1235 (1982); P. M. Radmore and P. L. Knight, Phys. Lett. **102A**, 180 (1984).

[13]D. A. Cardimona, M. G. Raymer, and C. R. Stroud, Jr., J. Phys. B **15**, 63 (1982); E. Kyrölä and J. H. Eberly, J. Chem. Phys. **82 (4)**, 1841 (1985).

[14]H. A. Bethe and E. E. Salpeter, *Quantum Mechanics of One- and Two-Electron Atoms* (Plenum, New York, 1977), p. 303.

[15]H. S. Antunes and L. Davidovich, Phys. Rev. Lett. **53**, 2283 (1984).

[16]P. W. Milonni, Phys. Rev. A **38**, 2682 (1988); P. W. Milonni and J. R. Ackerhalt, *ibid.* **39**, 1139 (1988).

[17]K. Gottfried, *Quantum Mechanics* (Benjamin, New York, 1966).